Atomistic view of impurities interacting with a quasi-one-dimensional charge density wave

Deok Mahn Oh and Han Woong Yeom*

Center for Artificial Low Dimensional Electronic Systems, Institute for Basic Science (IBS), Pohang 790-784, Korea
and Department of Physics, Pohang University of Science and Technology, Pohang 790-784, Korea

(Received 12 March 2016; revised manuscript received 25 May 2016; published 29 June 2016)

Atomistic details of the interaction of impurities with quasi-one-dimensional charge density wave (CDW) are revealed by scanning tunneling microscopy. Oxygen and pentacene adsorbates are utilized as strongly and weakly interacting impurities, respectively, on the well-known CDW state of the In atomic wire array on the Si(111) surface. Distinct CDW pinning configurations are identified for oxygen impurities with different atomic structures, indicating the strong pinning. The governing role of local strain field for the strong pinning is elucidated. In contrast, a few different pinning configurations occur for a unique adsorption structure of pentacene indicating a weak pinning. Pentacene molecules commonly induce characteristic phase shifts, which readily couple with other phase defects, in particular, solitons in order to avoid interwire phase misfits. This work provides the mechanism and methodology for the atomic scale control over phases, solitons, and domain boundaries of CDW.

DOI: 10.1103/PhysRevB.93.235448

I. INTRODUCTION

Physical properties of broken symmetry ground states, such as superconducting and charge density wave (CDW) states, are often drastically affected by impurities. In particular, impurities in CDW systems are related to the finite correlation length and the pinning of collective modes [1]. While the impurity-CDW interaction has been extensively studied with *microscopic* theoretical models [2–4], experimental approaches have largely replied on *macroscopic* or spatially averaging probes such as transport, optical, and x-ray measurements [5–7]. This has certainly imposed limitation on directly testing and developing theoretical concepts, such as weak or strong pinning of CDW phases and collective excitations [2–4]. In this respect, scanning tunneling microscopy (STM) can be an ideal tool since it can directly map local charge densities in atomic scale and identify individual impurities. For bulk quasi-two-dimensional (2D) CDW materials, a few pioneering STM studies reported impurity-induced CDW modifications such as the suppression of the CDW local amplitude and long range order and the pinning of domain boundaries [8–10]. However, individual bulk impurities were not clearly identified and characterized on the surface layers imaged by STM, which made it difficult to address the role of individual impurities and the pinning mechanism. For bulk quasi-1D CDW systems [11–13], there is no detailed STM study on the CDW-impurity interaction in the level of individual impurities, to the best of our knowledge.

In contrast to conventional 1D CDW materials, a surface CDW system such as the In atomic wire array on Si(111) can be an ideal playground for the atomic scale investigation of the CDW-impurity interaction due to the convenience of the impurity control and characterization as adsorbates. This system is composed of a monolayer of In self-organized into a wire array and exhibits a metal-insulator transition at a transition temperature (T_c) of 125 K into the CDW state [14,15]. Due to the double Peierls-distorted chain structure of a single wire, four degenerate CDW ground states are possible (Fig. 1), which lead to the Z_4 topological order [16]. While various adsorbates were already investigated on this system [17–25] for their atomic structures and their effects on the local or global change of T_c [17,20–23,26,27], no detailed study on the microscopic CDW perturbation by individual adsorbates is available.

In this work, we perform an extensive STM study for atomic and molecular impurities, oxygen [24,25] and pentacene (Pn, $C_{22}H_{14}$), adsorbed on the In atomic wire array above and below T_c. Below T_c, oxygen adatoms in different adsorption structures pin the phase of CDW distinctly, which can be well explained by the lattice strain fields imposed by adsorbates. These cases correspond to the strong impurity pinning [2–4]. In contrast, Pn molecules in a unique adsorption structure produce a few different CDW pinning configurations indicating a weak pinning. These pinning configurations, however, share the characteristic CDW phase shift. This phase shift easily traps other phase defects such as domain walls and solitons [16,28] in order to minimize the interwire interaction energy. The present results open a route toward controlling local phases, solitons, and domain walls of CDW systems.

II. EXPERIMENTS

The experiments were conducted using two commercial ultrahigh-vacuum STM's: a variable temperature STM (Omicron) for room temperature (RT) measurements and a cryogenic STM (Unisoku) at 78 K. An *n*-doped Si(111) surface was cleaned by repeated heating up to 1500 K. The In atomic wire array was prepared by depositing one monolayer of In onto a clean Si(111)7 × 7 surface at 570 K [14]. Oxygen atoms were carefully dosed at RT by backfilling the STM chamber with O_2 gas and pentacene molecules were deposited at RT through a homebuilt effusion cell.

III. RESULTS AND DISCUSSIONS

Above T_c, a single In atomic wire on Si(111) consists of two In zigzag chains as separated by Si zigzag chains with a 4 × 1 unit cell Fig. 1(a) [15,29]. In STM images, the protrusions with a periodicity of a_0 [the lattice constant

*yeom@postech.ac.kr

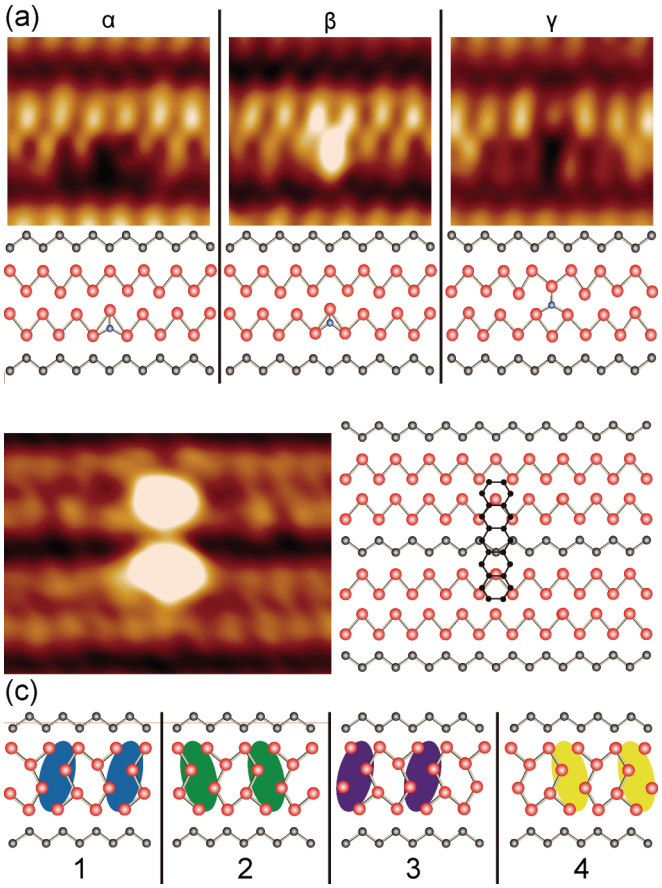

FIG. 1. (a) RT STM images of three different oxygen adsorption structures on the In atomic wires ($V_s = -0.4$ V, $I_t = 50$ pA, 2.8 nm × 2.3 nm) with corresponding structure models; red (gray) balls represent the indium (silicon) atoms and the blue balls oxygen adatoms. (b) Similar STM image of a pentacene adsorbate ($V_s = -0.2$ V, $I_t = 50$ pA, 43 nm × 24 nm) and the corresponding model. (c) Four different CDW ground state structures of In atomic wires at low temperature. Colored ovals represent CDW maxima shown in filled state STSM images.

of Si(111)] along In chains correspond to the sites between outer In atoms [Figs. 1(a) and 1(b)] [15]. Below T_c, the so-called hexagon structure is formed through a combination of dimerizations along two In zigzag chains [Fig. 1(c)] [30,31]. These hexagons are identified as oval protrusions in filled state STM images [colored ovals in Figs. 1(c) and 2] [32]. Due to the presence of double In zigzag chains and possible dimerization along each chain, four different CDW hexagon configurations are allowed to degenerate [Fig. 1(c)], which constitute a Z_4 topological insulator [16]. Three different characteristic solitons, or intrinsic phase shifters, are required to connect fourfold-degenerate ground states [16]. Under the interwire interaction, the CDW phase exhibits a 2D ordered 8×2 structure (Fig. 2) and phase defects (point defects) tend to aggregate to form connected domain boundaries between patches with different CDW ground states [Fig. 2(b)] (see Supplemental Material [33]).

The adsorption structures of oxygen adatoms on In atomic wires were detailed in the previous studies [24,25]. Figure 1(a) shows three different major adsorption structures identified at RT [24]. In the most popular adsorption structure, α, the oxygen adatom sits on the center of one In zigzag chain. The β structure has a similar site, but the oxygen adatom immerses below the In chain with extra bonding with Si atoms underneath. In the other structure γ, the oxygen adatom adsorbs between two In zigzag chains [24]. A typical STM image of In atomic wires with oxygen adsorbates below T_c is displayed in Fig. 2(a). The positions of adsorbates in different structures are indicated in Fig. 2(b). α adsorbates are dominating within the well ordered CDW domains and the minority species β and γ prefer to sit within the domain boundaries where the CDW phase shifts exist (see Supplemental Material [33]). This tendency is confirmed in a large set of STM images taken at different sample preparations.

The characteristic preference in adsorption sites are related to the different CDW phase pinning by oxygen adsorbates, which is revealed in the closeup images of Figs. 2(c), 2(d), and 2(e). The α adsorbate occupies only single CDW hexagon unit and does not cause further perturbation into the CDW lattice. In sharp contrast, β and γ structures flip the CDW hexagons without an exception to induce a characteristic phase shift. This unusual "flip" type of phase shift cannot occur in conventional commensurate CDW systems but is made possible by the presence of double Peierls chains within a single wire. That is, in the phase flip, only one of the zigzag chains has a phase shift [Figs. 3(b) and 3(c)] (see Supplemental Material [33]). This breaks the $\times 8$ interwire order, which would be energetically unfavorable. A majority of β and γ adsorbates, close to one-third of them, are found in domain boundaries of the 8×2 phase, while α without any phase shift is distributed over ordered domains. Since the adsorption occurs at RT well above T_c, we can conclude that the phase shifting adsorbates pin domain boundaries during cooling through T_c.

We note that the correspondence between phase shifts and oxygen adsorption structures is robust and unique. The standard model of the CDW-impurity interaction, the Fukuyama-Lee-Rice (FLR) model [1–4], considers only the incommensurate CDW with charged impurities to develop the strong and weak pinning concept. The difference between the incommensurate and the present commensurate CDW system is the degeneracy: infinitely degenerate CDW states of different phases for an incommensurate case but only four degenerate states for the present case. Although the phase degree of freedom is much limited, the unique CDW phase shift for each adsorbate structure indicates unambiguously the strong pinning case. The contrasting weak pinning case will be demonstrated below for pentacene adsorbates.

The underlying mechanism of the strong phase locking by oxygen adsorbates can be understood from their atomic structures. Deviating from the FLR model, the present oxygen adsorbates are not charged so as to exclude the possibility of Coulomb interaction [24]. However, the lattice distortion induced by adsorbates can affect the CDW state locally since CDW is based on the electron-lattice interaction. Figure 3 shows the displacements of In atoms due to the oxygen adsorption [yellow arrows in Fig. 3(a)] as revealed in the previous first-principles calculations [24]. The favorable dimerization configuration around each adsorption structure can straightforwardly be expected as shown in the figure (white

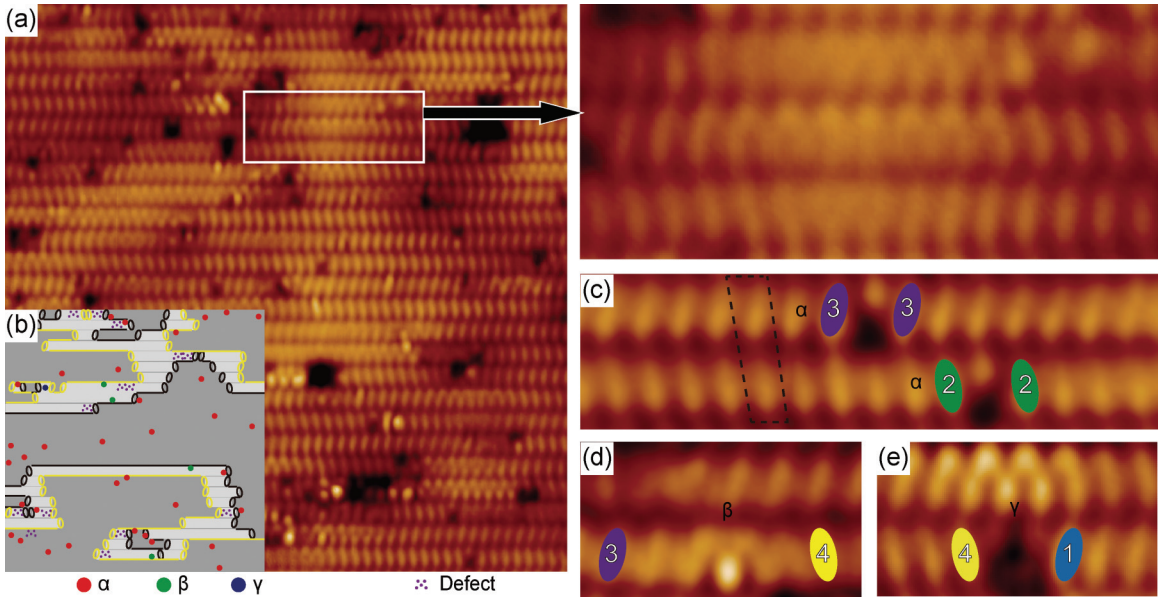

FIG. 2. (a) STM image of the In atomic wire array with oxygen adsorbates at 78 K ($V_s = -0.5$ V, $I_t = 10$ pA, and 34 nm × 34 nm in size). Edges of two 8 × 2 domains (black and yellow empty ovals), oxygens with α structure (red dots), oxygens with β structure (green dots), and oxygens with γ structure (blue dots) are marked with the domain boundary region (white) in (b). A part of the domain boundary region where the phase of CDW shifts gradually is enlarged. Popular intrinsic phase defects are indicated by symbols with five purple dots. (c), (d), and (e) Enlarged STM images and the CDW phase pinning configurations by α, β, and γ adsorption structures. The colored and numbered ovals indicate different CDW ground states defined in Fig. 1(b). The 8 × 2 unit cell of the 2D ordered CDW state is shown by a dashed box in (c).

arrows), which in fact matches nicely with the experimental observation: no phase shifts for α and the phase flip for β and γ structures. That is, the α structure has a local strain field coherent to the periodic lattice distortion of CDW, while the others do not. The coherent strain field of α adsorbates was recently found to induce local condensation of CDW around them above T_c [34]. In conclusion, oxygen impurities have strong pinning effects on the phase of CDW by their local strain fields, which in turn determines the pinning of CDW domain walls.

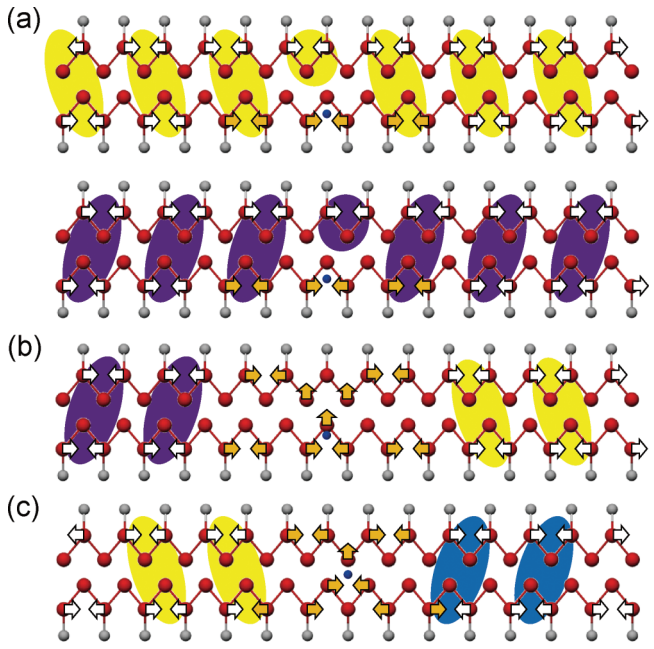

FIG. 3. Schematics of In atom displacements due to the oxygen adsorption (yellow arrows) and the compatible dimerization configuration for the CDW formation (white arrows) around (a) α, (b) β, and (c) γ oxygen adsorption structures. Colored ovals for different CDW ground states and the structure models are the same as those in Fig. 1.

In contrast to the strong pinning, a weakly interacting impurity would have various different phase pinning configurations based on four different CDW ground states. Figure 4(a) shows the filled state STM image of In atomic wires with Pn adsorbates. As reported previously, most of Pn adsorbates sit perpendicular to wires [35]. The molecules in filled state STM images exhibit enhanced contrast at both end phenyl rings, which is typical for Pn adsorbates on surfaces [36]. As shown in Fig. 1(b), the STM topography indicates that the central phenyl ring of Pn is symmetrically (mirror symmetric about the molecular axis) anchored on the Si zigzag chain. This is slightly different from the previous structure model of asymmetrically anchored molecules [35]. This model is ruled out here since we found only a symmetric structure for all molecules adsorbed perpendicular to wires. Since there is no dangling bond for In wires and Si zigzag chains on the surface, the strong covalent bonding interaction between adsorbate molecules and surface atoms is not possible *a priori*. In stark contrast, oxygen adsorbate molecules easily dissociate, as on many metal surfaces, to produce atomic adsorbates, which form strong bondings with surface atoms as inserted between In or In and Si atoms. That is, the weak and strong interaction of aromatic molecular and atomic adsorbates on the metallic surface of In/Si(111) is easily understood.

When the surface with Pn adsorbates is cooled below T_c, we find that molecules are distributed over both 8 × 2

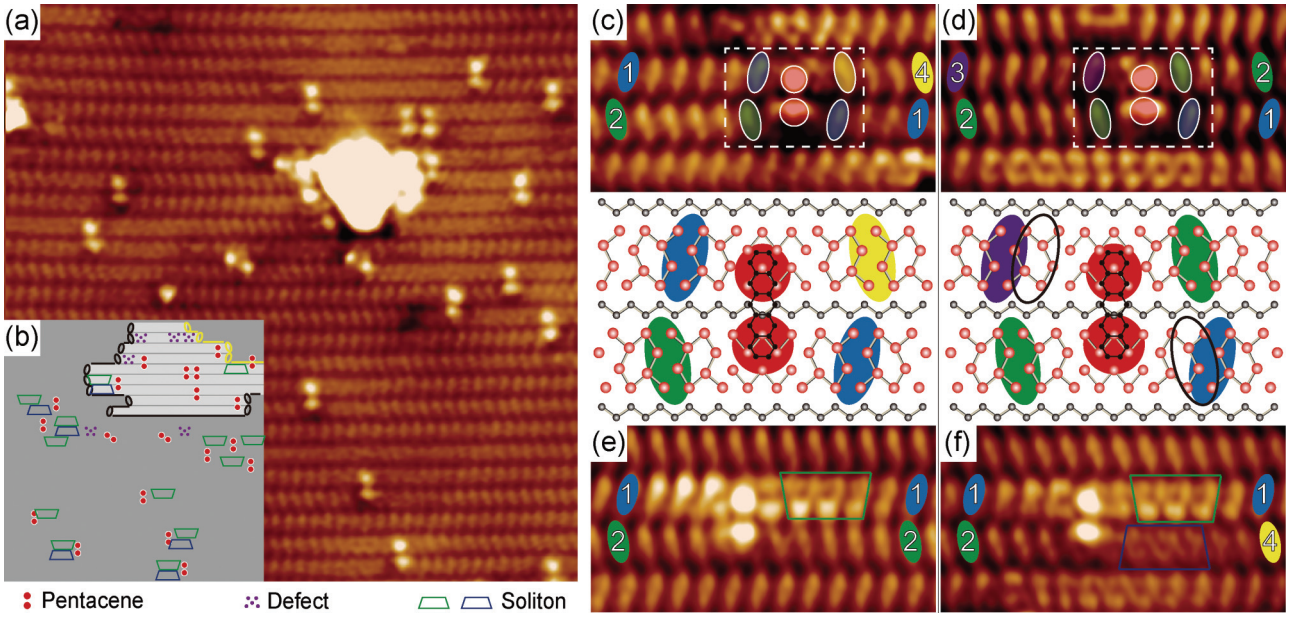

FIG. 4. (a) STM image of In atomic wires with pentacene adsorbates at 78 K ($V_s = -0.5$ V, $I_t = 10$ pA, and 33 nm × 33 nm in size). Edges of 8 × 2 domains (black and yellow empty ovals), domain boundary regions, pentacene molecules, and phase defects are marked in (b) in the same way as Fig. 2(b). The extra green and blue boxes indicate solitons stationary trapped and imaged. (c) and (d) Enlarged STM images (top) and CDW phase shift configurations with structure models (bottom and also overlaid in the STM images) for two particular Pn adsorbates within the domain boundary region. (e) and (f) Similar STM images for Pn adsorbates within the ordered CDW domains, which in most cases are coupled with solitons (green and blue boxes).

CDW domains and domain wall regions without a noticeable preference. This is distinct from oxygen adsorbates [Figs. 6(a) and 6(b)] and is related to the weak pinning interaction of Pn adsorbates and solitons. The enlarged STM images in Fig. 4 uncover the detailed relationship between CDW and a Pn adsorbate. Figures 4(c) and 4(d) show the STM images for Pn molecules within domain boundary regions. Here, one can find that Pn adsorbates induce two different phase shift configurations. It is obvious that the phase shift induced by Pn adsorbates is not unique, while most of them induce the phase flip as in the cases of β and γ oxygen structures. As discussed for oxygens, the phase flip induced by Pn molecules causes them to reside on domain boundary regions.

However, the substantial population of molecules within the ordered 8 × 2 domains, then, looks very much strange. We note very interestingly that most of these molecules are attached with solitons as indicated in Fig. 4(b) and detailed in Figs. 4(e) and 4(f). The molecule shown in Fig. 4(f) is coupled with two soliton phase shifters. These solitons eliminate the local phase shift induced by the adsorbate, which obviously allow the Pn adsorbate to be located within the ordered domain without causing an interwire phase misfit of a large energy cost. For the other molecule shown in Fig. 4(e), the soliton is attached only in the upper wire but there is no phase shift in the bottom wire. This case is not rare as shown in Fig. 4(b) and corroborates further that the phase pinning by Pn adsorbates is weak and clearly contrasted with the case of the strong pinning by oxygen adsorbates. However, the weak pinning nature of Pn molecular adsorbates has a deviating feature from the weak pinning of an incommensurate CDW system formulated in the FLR model [1–3]. In the FLR model, the weak pinning leads to the excitation of "collective" modes. Such collective phase modes are not possible in a commensurate system. We, however, think that the excitation of the collective mode is in line with the trapping of solitons observed here in a sense to gradually relax the local phase shift induced by an impurity.

The microscopic pinning mechanism of Pn could be very much different from that of oxygen adsorbates since a Pn molecule has no direct covalent bonding with surface atoms to induce any substantial lattice strain. While the clear confirmation is beyond the scope of the present work, we note that the observed CDW hexagon configurations [summarized in Fig. 4(d)] can roughly be explained when we assume a hindered area of the CDW maxima (ovals) around a molecule as depicted in the figure. Since the charge density maxima of CDW are basically the bonding state of the Peierls dimerization, we suggest that the pinning in this case can be explained in a similar way to the steric hinderance between molecules; the avoided overlap of molecular orbitals and the CDW bonding (or antibonding) orbitals. We finally comment on the soliton trapping of Pn adsorbates. It is fully shown above that the impurities with phase shifts such as Pn and β and γ oxygen structures has strong tendency to couple with other phase shifters such as domain boundaries or solitons. This tendency can qualitatively be understood by the presence of the substantial interwire interaction to make the interwire phase misfit costly. In turn, this interwire interaction and the phase shifting impurities apparently provide substantial pinning potentials for domain boundaries and solitons, which can be exploited further.

In the present work, we show the weak and strong pinning of CDW by individual atomic scale impurities and address the underlying mechanism based on the local lattice strain field and the interwire interaction. The phase shifts induced by

impurities in turn couple readily with domain boundaries and solitons. The pinning phenomena revealed here for CDW, its domain boundaries, and solitons by adsorbate impurities pave the way to microscopic control over this interesting quantum state of solids and its local excitations.

ACKNOWLEDGMENT

This work was supported by Institute for Basic Science (Grant No. IBS-R014-D1).

[1] G. Grüner, *Density Waves in Solids* (Addison-Wesley Publishing Company, Advanced Book Program, Redwood City, CA, 1994).
[2] H. Fukuyama and P. A. Lee, Phys. Rev. B **17**, 535 (1978).
[3] P. A. Lee and T. M. Rice, Phys. Rev. B **19**, 3970 (1979).
[4] I. Tütto and A. Zawadowski, Phys. Rev. B **32**, 2449 (1985).
[5] D. Reagor and G. Grüner, Phys. Rev. B **39**, 7626 (1989).
[6] L. Degiorgi, B. Alavi, G. Mihály, and G. Grüner, Phys. Rev. B **44**, 7808 (1991).
[7] E. Sweetland, C.-Y. Tsai, B. A. Wintner, J. D. Brock, and R. E. Thorne, Phys. Rev. Lett. **65**, 3165 (1990).
[8] X.-L. Wu, P. Zhou, and C. M. Lieber, Phys. Rev. Lett. **61**, 2604 (1988).
[9] H. Dai, H. Chen, and C. M. Lieber, Phys. Rev. Lett. **66**, 3183 (1991).
[10] H. Chen, X. L. Wu, and C. M. Lieber, J. Am. Chem. Soc. **112**, 3326 (1990).
[11] M. P. Nikiforov, A. F. Isakovic, and D. A. Bonnell, Phys. Rev. B **76**, 033104 (2007).
[12] C. Brun, Z.-Z. Wang, P. Monceau, and S. Brazovskii, Phys. Rev. Lett. **104**, 256403 (2010).
[13] T. Nishiguchi, M. Kageshima, N. Ara-Kato, and A. Kawazu, Phys. Rev. Lett. **81**, 3187 (1998).
[14] H. W. Yeom, S. Takeda, E. Rotenberg, I. Matsuda, K. Horikoshi, J. Schaefer, C. M. Lee, S. D. Kevan, T. Ohta, T. Nagao, and S. Hasegawa, Phys. Rev. Lett. **82**, 4898 (1999).
[15] J.-H. Cho, D.-H. Oh, K. S. Kim, and L. Kleinman, Phys. Rev. B **64**, 235302 (2001).
[16] S. Cheon, T.-H. Kim, S.-H. Lee, and H. W. Yeom, Science **350**, 182 (2015).
[17] S. V. Ryjkov, T. Nagao, V. G. Lifshits, and S. Hasegawa, Surf. Sci. **488**, 15 (2001).
[18] G. Lee, S.-Y. Yu, H. Kim, and J.-Y. Koo, Phys. Rev. B **70**, 121304 (2004).
[19] C. Liu, T. Uchihashi, and T. Nakayama, Phys. Rev. Lett. **101**, 146104 (2008).
[20] G. Lee, S.-Y. Yu, H. Shim, W. Lee, and J.-Y. Koo, Phys. Rev. B **80**, 075411 (2009).
[21] H. Morikawa, C. C. Hwang, and H. W. Yeom, Phys. Rev. B **81**, 075401 (2010).
[22] T. Shibasaki, N. Nagamura, T. Hirahara, H. Okino, S. Yamazaki, W. Lee, H. Shim, R. Hobara, I. Matsuda, G. Lee, and S. Hasegawa, Phys. Rev. B **81**, 035314 (2010).
[23] S. H. Uhm and H. W. Yeom, Phys. Rev. B **88**, 165419 (2013).
[24] D. M. Oh, S. Wippermann, W. G. Schmidt, and H. W. Yeom, Phys. Rev. B **90**, 155432 (2014).
[25] H. Shim, H. Lim, Y. Kim, S. Kim, G. Lee, H.-K. Kim, C. Kim, and H. Kim, Phys. Rev. B **90**, 035420 (2014).
[26] M. Hupalo, T.-L. Chan, C. Z. Wang, K.-M. Ho, and M. C. Tringides, Phys. Rev. B **76**, 045415 (2007).
[27] H. Zhang, F. Ming, H.-J. Kim, H. Zhu, Q. Zhang, H. H. Weitering, X. Xiao, C. Zeng, J.-H. Cho, and Z. Zhang, Phys. Rev. Lett. **113**, 196802 (2014).
[28] T.-H. Kim and H. W. Yeom, Phys. Rev. Lett. **109**, 246802 (2012).
[29] O. Bunk, G. Falkenberg, J. H. Zeysing, L. Lottermoser, R. L. Johnson, M. Nielsen, F. Berg-Rasmussen, J. Baker, and R. Feidenhans'l, Phys. Rev. B **59**, 12228 (1999).
[30] C. González, J. Ortega, and F. Flores, New J. Phys. **7**, 100 (2005).
[31] A. A. Stekolnikov, K. Seino, F. Bechstedt, S. Wippermann, W. G. Schmidt, A. Calzolari, and M. Buongiorno Nardelli, Phys. Rev. Lett. **98**, 026105 (2007).
[32] C. González, J. Guo, J. Ortega, F. Flores, and H. H. Weitering, Phys. Rev. Lett. **102**, 115501 (2009).
[33] See Supplemental Material at http://link.aps.org/supplemental/10.1103/PhysRevB.93.235448 for the details of the phase shifted CDW configurations.
[34] H. W. Yeom, D. M. Oh, S. Wippermann, and W. G. Schmidt, ACS Nano **10**, 810 (2016).
[35] H. Zhang, Y. Li, B. Li, X. Fang, H. Ji, B. Wang, C. Zeng, and J. Hou, Surf. Sci. **603**, L70 (2009).
[36] J. Lagoute, K. Kanisawa, and S. Fölsch, Phys. Rev. B **70**, 245415 (2004).